Molecular Dynamics Simulation Study on the Possible Factors Affecting Stability of ODS Steel

M.Mustafa Azeem, Zhongyu Li , Qingyu Wang and Abid Hussian

College of Nuclear Science & Technology, Harbin Engineering University, 150001, P.R China.

lizy820601@163.com (Zhongyu Li); mustafa@hrbeu.edu.cn (M.Mustafa Azeem)

Abstract. Oxide-dispersed-strengthened (ODS) steel has excellent mechanical, thermodynamic and radiation resistant properties, which makes it an important candidate material for high-temperature reactors applications. Radiation stability of oxide is very important to study at the atomic level. In present case molecular dynamics (MD) simulation is used to study stabilities of Y_2O_3 particles in ODS steel as a function of particle sizes. The size dependence is obvious for particle sizes larger than 2.8 nm. Furthermore, the stabilities depend on charges of Y and O atoms.

1. Introduction

The structural materials in nuclear reactors have degradation caused by irradiation damage. Research on advanced fission and fusion reactors put forward higher requirements for the safety and economy of reactors, which lead to critical needs for materials of better performance [1,2,3,4]. So far candidate materials for reactor-core components include nickel-based alloys, austenitic stainless steels, ferrite / martensitic steels, and oxide dispersion strengthening (ODS) steels [5]. ODS steel is unique for high temperature applications due to their high creep resistances from embedded oxide particles of nanometre sizes [3,5,6,7,8]. In order to further optimize ODS steels, MD simulations are needed to study atomic scale details of the structural evolution of oxide particles under high temperatures. The thermal stabilities of particles are important for their applications in high temperature fast reactors. In present study some possible factors affecting the stability of ODS are discussed by MD simulation method.

2. Modeling procedure

The dispersoids in ODS steels are typically Y-Ti-O oxide. As a model material, Y_2O_3 embedded Fe is simulated by using LAMMPS (Large scale Atomic Molecular Massively Parallel Simulator)[9]. The interatomic potentials are described by hybrid potentials from Hammond et al [10]. The potential is linked to Ziegler-Biersack-Littmark (ZBL) potential for short-range interactions [11]. Simulation cell has dimensions of $22nm_x22nm_x22nm$ and has one oxide particle of size 5 nm embedded at the center. Periodic boundary conditions are applied on all sides. The cell is relaxed initially by isobaric-isothermal ensemble NPT for 100ps, followed by microcanonical ensemble NVE for 100ps at 300K. Figure 1 shows the cell structure. The red color represents O atoms, and green color for Y atoms, and the purple color for Fe atoms. The cell contains 1015597 atoms including 21550 O atoms and 14086 Y atoms. The Open Visualization Tool (OVITO) [12] is used for visualization of LAMMPS output.

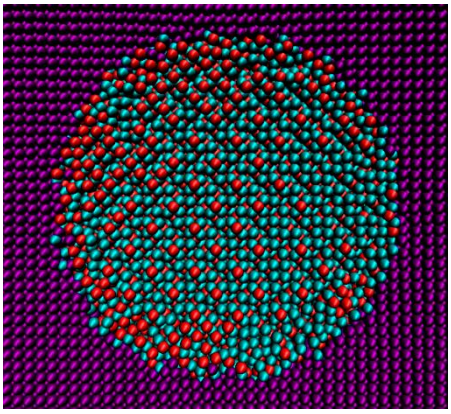

Figure 1. Structure of model after thermal relaxation with Fe embedded 5nm oxide at 300K.

3. Results and discussion

Figure 2 shows the temperature changes of the system as a function of time. The initial temperature is 300K. With increasing time, the temperature rises up and then drops down to reach a saturated, value at a time longer than about 20 ps. Figure 3 shows a variation of total energy vs. time for a thermal relaxation at 300K. The trend of the total energy changes is roughly the same as the change of temperature as shown in Figure 2.After relaxation longer than 20ps, the energy fluctuations are very small, which suggests the system has reached an equilibrium state. We find that thermal stability of the oxide particle at a longer time depends on the factors other than temperatures, as explained below.

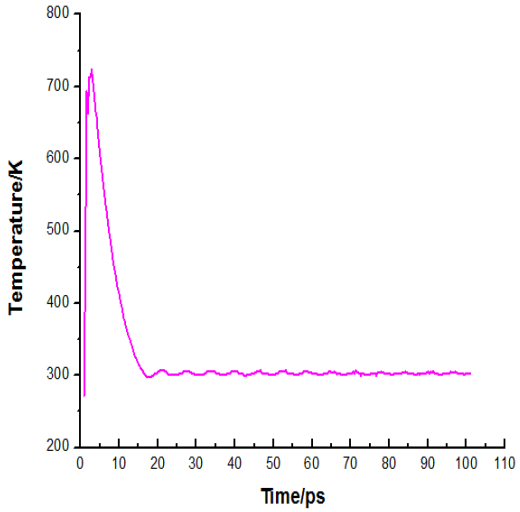

Figure 2. Temperature changes of the cell as a function of time for the thermal relaxation at 300K.

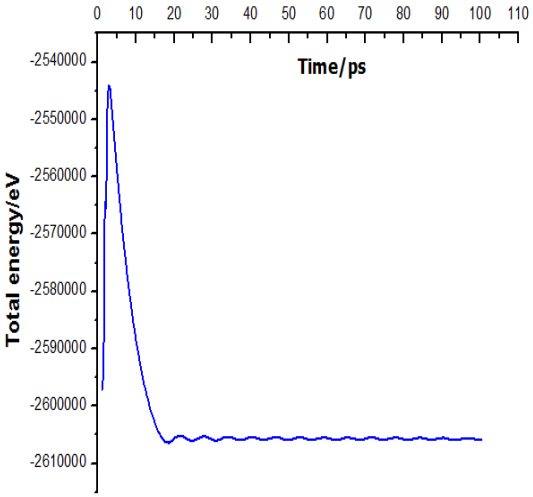

Figure 3. Energy changes as a function of time for the cell relaxed at 300K.

3.1. Factors affecting the stability

3.1.1. Dependence on size of the oxide. MD simulations are performed by changing the radii of oxide particles as shown in Figure 4. For small oxide particle sizes of 1.5 nm and 2 nm, MD simulations show non-spherical configurations and amorphous-like structures after thermal relaxation at 300K. At a radius of 2.8 nm, atomic arrangement starts to become spherical and ordered. At larger sizes crystallinity of oxide particles is further improved. Only at the interfaces of oxide particle and Fe

matrix highly disorder regions exist. Clearly, the size plays an important role to influence stabilities of oxide particles. This can be understood by a large interface-to-volume ratio of small oxide particles. A defective interface has high energy [13-16]. Large interface-to-volume ratios may increase the system energy of the oxide particle to a level exceeding the critical energy for amorphization [17-19].

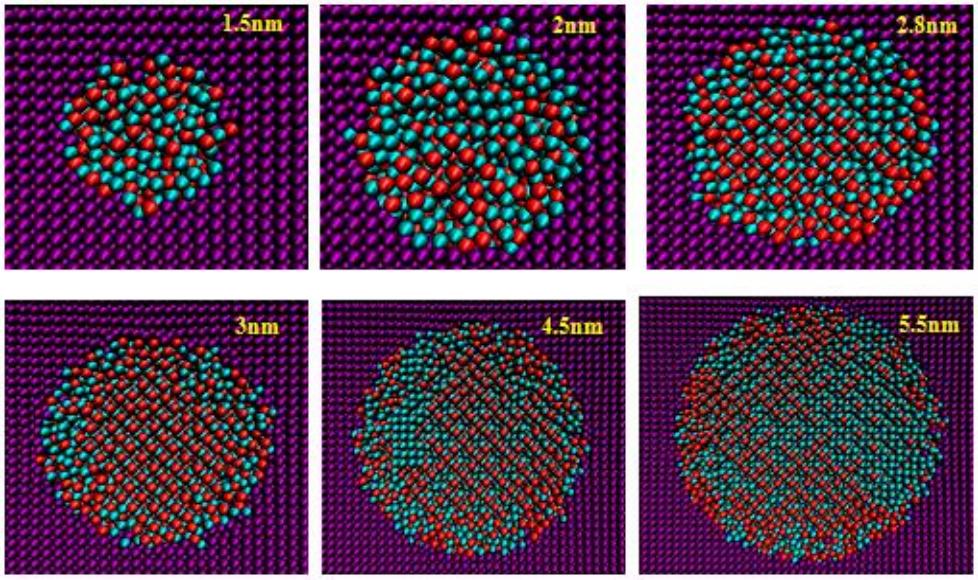

Figure 4. Snapshot of oxide particles of different radii at 300K.

Figure 5 plots the atomic energy per atom as a function of oxide particle sizes. When oxide sizes are 1nm and 1.5nm, the total numbers of Y and O atoms are 287 are 943 and average atomic energies of Y and O atoms are -15.67 eV and -15.37 eV respectively. When oxide size is 2.0 nm, the total number of Y and O atoms is 2227, and the average atomic energy of Y and O is -0.0023 eV. At 2.5nm, the total number of Y and O atoms is 4,392, and the average atomic energy of Y and O is -0.0028 eV. At 2.8nm, the total number of Y and O atoms is 6132, and the average atomic energy of Y and O atoms is -14.93 eV. At 3nm, the total number of Y and O atoms is 7584, and the average atomic energy of Y and O atoms is -14.96 eV. Our modeling shows that at sizes at 2.8 nm and larger, average atomic energy reaches saturation.

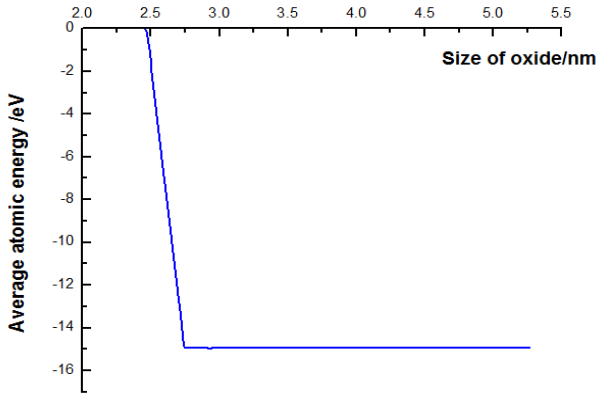

Figure 5. Variation of average atomic energy as a function of oxide particle sizes.

3.1.2. Influence of charge. Under the same relaxation temperatures, we further tested the effect of Y/O charge ratios to the oxide particle stability. For charges of Zy=2.55 (for Y) and Zo=-1.7 (for O), the oxide particle shows instability and the generation of cavity near the interface (as shown in Figure. 6a). In a comparison, for charge values of Zy=1.66 and Zo=-1.11,relaxed structure looks stable without any cavity as shown in Figure. 6b [20,21].

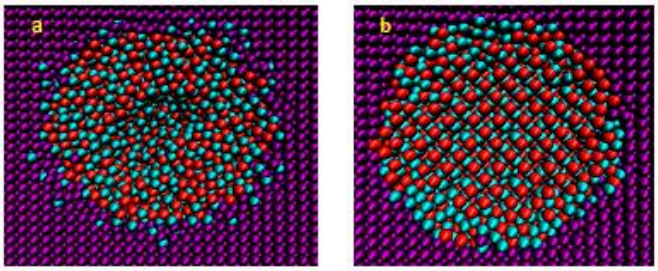

Figure 6. Snapshot of a 2.8nm oxide at 300Kwith different Y/O charges.

3.1.3. Influence of temperature. Due to the importance of temperature in reactor application, we further tested stabilities of oxide particle of 2.8 nm size at 300K, 900K, 1200K, and 1500K. The charge values of Zy=1.66 and Zo=-1.11 are used for the best stabilities. Figure 7 compares the oxide particle morphologies as a function of temperatures.

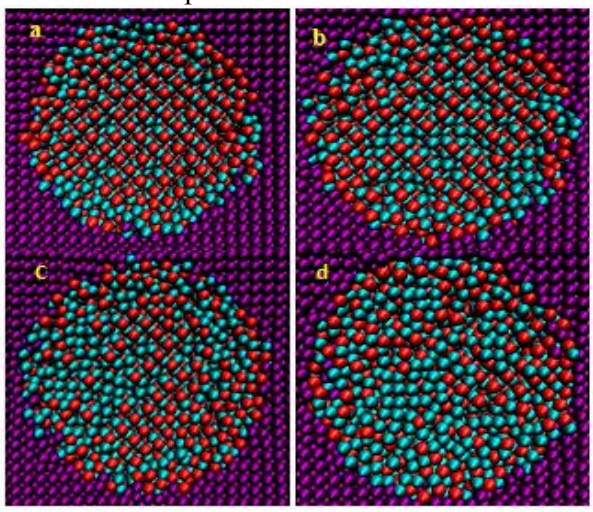

Figure 7. Structural morphologies of oxide particle of 2.8nm size at temperatures of (a) 300K (b) 900K (c) 1200K and (d) 1500 K respectively.

The critical stability sizes are found to increase with increasing temperature. Figure 8 shows structural morphologies of oxide particles of 2.5nm, 2.8nm, 3nm respectively, at 900K. It shows that at the size of 3nm (Figure. 8c) oxide particle still maintain crystallinity.

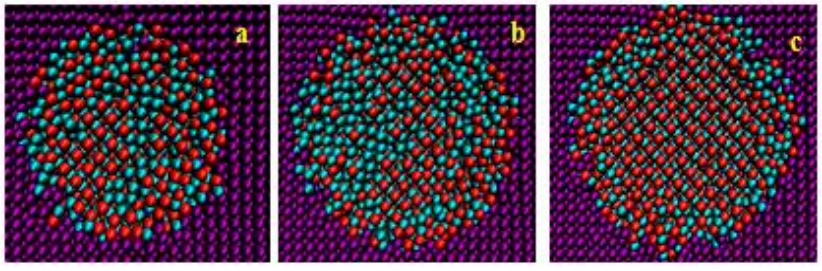

Figure 8. Structural morphology for oxide with sizes (a) 2.5nm, (b) 2.8nm, (c) 3 nm at 900K.

Figure 9 plots the critical stability sizes as a function of temperatures. The higher the temperature, the larger the size required to reach stability. For realistic applications which involves either high temperatures during the materials processing or high temperatures during operations, it is needed to consider this size effects and introduce stabilize particles. On the other hand, we hypothesize that amorphous or unstable oxide particles may get dissolved into the matrix and promote nucleation of new oxide particles and growth of these particles into the favorable size ranges.

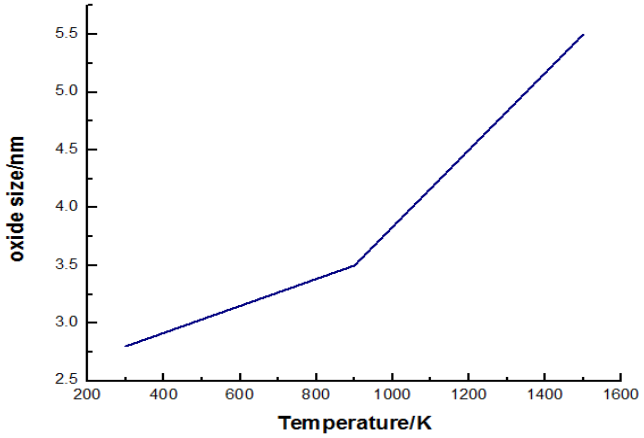

Figure 9. Critical sizes for structural stability as a function of temperature.

4. Conclusion

Through systematic modeling of oxide particles in Fe under various temperatures and as a function of sizes, we found that there is an existence of critical sizes below which oxide particles will become unstable and amorphized. This critical stability size increases with increasing temperatures. The oxide particle stability is sensitive to charge/ionization levels of Y and O atoms. There is an existence of optimized charge ratios for obtaining structural stability.

Acknowledgments

The authors greatly appreciate the financial support from the International Exchange Program of Harbin Engineering University P.R China & Chinese Scholarship Council (CSC) for their international scholarship program. Qingyu Wang acknowledges the support from National Science Foundation of China (Grant No.11505037).

References

[1] Muroga T, Gasparotto M and Zinkle S J 2002 *Fusion Eng. and Des.* 61–62 13–25.
[2] Yvon P and Carré F 2009 *J. Nucl. Mater*.385 217–22.
[3] Zinkle S J and Busby J T 2009 *Mater. Today* 12 12–19.
[4] Yvon P, Le Flem M, Cabet C and Seran J L 2015 *Nucl. Eng. Des*.294 161–9.
[5] Azevedo C R F 2011 *Eng. Fail. Anal*.181943–62.
[6] Murty K L and Charit I 2008 J. *Nucl. Mater*. 383 189–95.
[7] Klueh R L,Shingledecker J P,Swindeman R W,Hoelzer D T 2005 *J. Nucl. Mater*.341 103–14
[8] Klueh R L and Nelson A T 2007 *J. Nucl. Mater.*371 37–52.
[9] Plimpton S 1995 *J. Chem. Phys*. 1171–19.
[10] Hammond K D,Lee Voigt H-J,Marus L A,Juslin N and Wirth B D 2013 *J.Phys:Condens.Matter* 25 55402–13.
[11] Biersack J P and Ziegler J F 1982 *Nucl. Instruments Methods* 194 93–100.
[12] Stukowski A 2010 *Simul.Mater. Sci. Eng.*18 15012.
[13] Lu C et al 2016. *Sci. Rep*. 6 19994.
[14] Brodrick J, Hepburn D J and Ackland G J 2013 *J. Nucl. Mater* 445 291–7.

[15] Backhaus-Ricoult M 2003 *Physical Chemistry Chemical. Phys*. 5 2174–82.
[16] Becquart C S and Domain C 2011 *Metall. Mater. Trans. A*42 852–70.
[17] S. Rogozhkin et al 2016 *Nucl. Mater. Energy* 9 66–74.
[18] Beyerlein I J, Demkowicz M J, Misra A and Uberuaga B P 2015 *Prog. Mater. Sci.*74 125–210
[19] Demkowicz M J, Bellon P and Wirth B D 2010 *MRS Bull*. 35 992–8
[20] A M Mustafa, Z Li, Lin Shao 2017 *ASME 25th Int. Conf.on Nuclear Eng. ICONE-25* (China) 5 1-5.
[21] M M Azeem, Z Li, Q Wang, Q M N Amjad, M Zubair and O M H Ahmed 2018 *IEEE* 15th*Int. Bhurban Conf. on Applied Sci. & Tech.IBCAST* (Pakistan) 12–15.